TRUE BOND GRAPH FORMULATION FOR COMPRESSIBLE THERMOFLUID DUCT FLOWS

J. L. Baliño

Departamento de Engenharia Mecânica, Escola Politécnica, Universidade de São Paulo, São Paulo, Brazil

jlbalino@usp.br

ABSTRACT

In this paper a bond graph methodology described in a previous contribution (Baliño *et al.*, 2006) is used to model compressible one-dimensional pipe flows with rigid walls. Physical effects compatible with the one-dimensional approximation such as shear wall and normal stresses, wall and axial heat conduction and flow passage area changes can be modeled naturally. Nodal vectors of mass, velocity and entropy are defined as bond graph state variables. The state equations and the coupling between the inertial and entropy ports are modeled with true bond graph elements.

Keywords: compressible fluid flow, true bond graphs, numerical methods, Finite Elements, CFD

1. INTRODUCTION

The bond graph (BG) formalism allows for a systematic approach for representing and analyzing dynamic lumped parameter systems (Borutzky, 2010; Karnopp *et al.*, 2012). Dynamic systems of concentrated parameters belonging to different fields of knowledge like Electrodynamics, Solid Mechanics or Fluid Mechanics can be described in terms of a finite number of variables and basic elements.

Fluid Dynamics is a challenging area for bondgraphers, because these systems are rigorously described by non-linear partial differential equations (PDEs) with important spatial effects and exhibit couplings between different energy domains.

In order to solve multidimensional problems with the aid of computer programs, it is important that these models can be implemented numerically. This task, main concern of the area of Computational Fluid Dynamics (CFD), is performed by systematically discretizing the continuum, that is, by replacing the continuous variables by a combination of a finite set of nodal values and interpolating functions.

The first attempt to apply BG in fluid dynamic systems with a systematic spatial discretization of flow fields, typical of CFD problems, appeared in Fahrenthold & Venkataraman (1996). A one-dimensional compressible flow was considered, although the formulation was restricted to prescribed shape functions and nodalization. Besides, heat conduction (which leads to advection-diffusion problems) was not modeled.

In Baliño *et al.* (2001, 2006) a theoretical development of a general BG approach for CFD was presented. Density, entropy per unit volume and velocity were used as discretized variables for single-phase, single component flows. Time-dependent nodal values and interpolation functions were introduced to represent the flow field. Nodal vectors of mass, entropy and velocity were defined as BG state variables. It was shown that the system total energy can be represented as a three-port IC-field. The conservation of linear momentum for the nodal velocity is represented at the inertial port, while mass and thermal energy conservation equations are represented at the capacitive ports. All kind of boundary conditions are handled consistently and can be represented as generalized modulated sources.

In Baliño (2009) the methodology was applied to model multidimensional incompressible flows. The distinctive characteristic of these flows is the role of pressure, which does not behave as a state variable but as a function that ensures that the resulting velocity field has divergence zero. The system of equations for the momentum equation and for the incompressibility restriction is coincident with the one obtained using the Galerkin formulation of the problem in the Finite Element Method, while for the thermal energy equation a Petrov-Galerkin formulation is used. The integral incompressibility restriction was derived based on the integral conservation of mechanical energy. All kind of boundary conditions are handled consistently and can be represented as generalized effort or flow sources for the velocity and entropy balance equations. A procedure for causality assignment was derived for the resulting graph, satisfying the Second Principle of Thermodynamics.

The methodology presented in Baliño *et al.* (2006); Baliño (2009) has the following characteristics, briefly described as follows:

a) The total energy rate per unit volume is represented at the continuum level by a summation of products of generalized efforts times flow per unit volume variables.

b) The balance equations, corresponding to each one of the terms appearing in the total energy rate per unit volume, are derived based on the PDEs representing the conservation laws; in this way, all physical effects can naturally be taken into account.

c) The balance equations show the power structure of the system at the continuum level; coupling between the different energy domains appears naturally as terms with opposite signs in the corresponding balance equations.

d) The discretization is made in terms of nodal values and interpolation and weight functions; in this way, all the properties are kept at the discretized level, resulting generalized effort and flow variables characteristic of true BG.

Consequently, the formulation links two areas, namely the BG methodology and CFD. It is interesting to see that, although temperature and entropy rate are the natural BG variables in thermal problems, bondgraphers resort to pseudo-BG or other non-BG elements when modeling thermofluid flow problems, as if there were some intrinsic difficulty in incorporating naturally all the relevant physical effects.

The calculation of pressure and flow distributions is very important for the design of pipeline networks. For engineering purposes, pipe flows are studied using the one-dimensional approximation, in which the non-uniformity of any flow parameter across the flow passage area can be neglected. In this case, suitable average values of all flow parameters are functions of time and the coordinate along the length of the pipe. Small changes in pipe direction and cross sectional area are allowed, as long as they do not create flow separation or secondary flows. In order to reintroduce the information lost in the averaging process, closure laws for wall momentum and heat transfer, as well as suitable profile correction factors, must be defined. The behavior of pipe flow is governed mainly by the Reynolds number, measuring the relative influence of inertial and viscous forces.

Incompressible pipe flow is a classic branch of Hydraulics which addresses liquid and low velocity gas flows within a closed conduit, without a free surface. The methodology presented in Baliño *et al.* (2006) was applied to incompressible one-dimensional pipe flows in Baliño (2006b); transient advective and advective-diffusive problems were successfully simulated in Pellegrini & Baliño (2014).

When the fluid velocity is comparable to the speed of sound, compressibility effects become important (Schapiro, 1953). Mass, momentum and energy conservation equations are coupled and an equation of state is needed to close the problem. As this condition is frequently encountered in gas systems (usually the fluid is considered as an ideal gas), the object of study is known as gas dynamics. Basic studies of compressible pipe flows assume that viscous and heat transfer effects are negligible, leading to isentropic flows; performance of converging and converging-diverging nozzles are typical examples studied with this approximation. More sophisticated studies take into account wall shear stresses (Fanno flows) and heating/cooling (Rayleigh flows). Distinctive effects in compressible flows are the limitation of the mass flow rate when the local velocity equals the sound of speed (choking) and existence of very thin discontinuities in the flow properties, associated to irreversibilities (normal shock waves).

The motivation of this paper is the application of the methodology presented in Baliño *et al.* (2006) to model compressible one-dimensional pipe flows; as this flow is very rich in specific applications, numerical benchmarks are left for a separate contribution. Results for the shock tube problem were presented in Gandolfo Raso *et al.* (2001); this paper extends the methodology to one-dimensional flows with area changes, wall heat transfer and wall shear stress dissipation.

The paper is organized as follows: the formulation at the continuum level, presenting the independent variables, associated potentials, conservation and balance equations is presented in Section 2.; the formulation at the discrete level, presenting the nodal vectors of the state variables, associated nodal vectors of potentials and state equations is presented in Section 3.; finally the system BG, showing the power couplings between the different ports and the different sources, is presented in Section 4.

2. CONTINUUM LEVEL FORMULATION

Let us consider the geometry of Fig. 1. For the one-dimensional approximation, the independent variables are functions of position x and time t, whereas the flow passage area A is a slowly varying function of position.

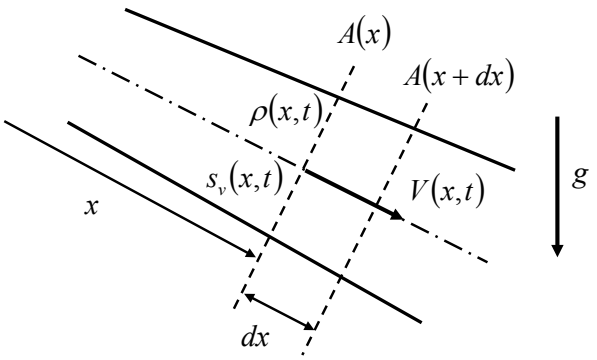

Figure 1: Control volume for one-dimensional compressible duct flow.

2.1 Total energy

The total energy per unit volume e_v ($e_v = \rho\,\hat{e}$, where ρ is the density and $\hat{e}$ is the total energy per unit mass) is defined as the sum of the internal energy per unit volume u_v ($u_v = \rho\,\hat{u}$, where $\hat{u}$ is the internal energy per unit mass) and the kinetic coenergy per unit volume t_v^*:

$$e_v = u_v\,(\rho,\, s_v) + t_v^* \tag{1}$$

It is assumed that the internal energy per unit volume is a function of density and entropy per unit volume s_v ($s_v = \rho\,\hat{s}$, where $\hat{s}$ is the entropy per unit mass). The kinetic coenergy per unit volume is defined as:

$$t_v^* = \frac{1}{2}\,\rho\,V^2 \tag{2}$$

where V is the velocity. The following potentials are defined:

$$p_v = \left(\frac{\partial t_v^*}{\partial V}\right)_\rho = \rho\,V \tag{3}$$

$$\kappa = \left(\frac{\partial t_v^*}{\partial \rho}\right)_V = \frac{1}{2} V^2 \tag{4}$$

$$\theta = \left(\frac{\partial u_v}{\partial s_v}\right)_\rho \tag{5}$$

$$\psi = \left(\frac{\partial u_v}{\partial \rho}\right)_{s_v} = \frac{1}{\rho}\left(u_v + P - \theta\, s_v\right) \tag{6}$$

where $\boldsymbol{p}_v$, κ, θ, ψ and P are respectively the linear momentum per unit volume, the kinetic coenergy per unit mass, the absolute temperature, the Gibbs free energy per unit mass and the absolute pressure. The time derivative of the total energy per unit volume can be written as:

$$\frac{\partial e_v}{\partial t} = (\psi + \kappa)\frac{\partial \rho}{\partial t} + p_v \frac{\partial V}{\partial t} + \theta \frac{\partial s_v}{\partial t} \tag{7}$$

It can be shown (Baliño *et al.*, 2006) that the constitutive relations $\psi+\kappa$, p_v and θ satisfy the Maxwell relations (Callen, 1960).

For the particular case of an ideal gas, the internal energy per unit volume and thermodynamic potentials result:

$$u_v = \rho\, c_v\, \theta \tag{8}$$

$$P = \rho\, c_v\, (\gamma - 1)\, \theta \tag{9}$$

$$\psi = \left(\gamma\, c_v - \frac{s_v}{\rho}\right)\theta \tag{10}$$

$$\theta = \theta_R \left(\frac{\rho}{\rho_R}\right)^{\gamma-1} \exp\left(\frac{s_v}{\rho\, c_v}\right) \tag{11}$$

where c_v is the constant volume specific heat, γ is the heat capacity ratio and ρ_R and θ_R are respectively the reference density and temperature for which the entropy per unit volume is zero.

2.2 Conservation and balance equations

Neglecting property changes across the flow passage area, the mass, linear momentum in the flow direction coordinate x and thermal energy conservation equations can be integrated over the flow passage area, resulting:

$$\frac{\partial \rho}{\partial t} = -\frac{1}{A}\frac{\partial}{\partial x}\left(\rho\, V\, A\right) \tag{12}$$

$$\rho \frac{\partial V}{\partial t} = \frac{1}{A}\frac{\partial}{\partial x}\left(\tau_{xx}\, A\right) - \rho\, V \frac{\partial V}{\partial x} - \frac{\partial P}{\partial x} - \tau_{wx}\frac{\mathcal{P}_w}{A} + \rho\, g_x \tag{13}$$

$$\begin{aligned}\rho \frac{\partial \hat{u}}{\partial t} = &-\frac{1}{A}\frac{\partial}{\partial x}\left(q_x\, A\right) - q_w \frac{\mathcal{P}_h}{A} - \rho\, V \frac{\partial \hat{u}}{\partial x} + \tau_{xx}\frac{\partial V}{\partial x} \\ &+ \tau_{wx}\, V \frac{\mathcal{P}_w}{A} - P\frac{1}{A}\frac{\partial}{\partial x}\left(V\, A\right) + \rho\, \Phi\end{aligned} \tag{14}$$

where τ_{wx} and τ_{xx} are respectively the viscous wall shear stress and the viscous normal stress, $\mathcal{P}_w$ and $\mathcal{P}_h$ are respectively the wetted and heated perimeters, g_x is the gravity acceleration component in the flow direction, q_w and q_x are respectively the wall and axial heat flux and Φ is the heat source per unit mass. The wall shear stress and wall heat flux can be modeled as:

$$\tau_{wx} = \frac{1}{8} f\, \rho\, V\, |V| \tag{15}$$

$$q_w = -H\left(\theta_w - \theta\right) \tag{16}$$

where f is the Darcy friction factor, H is the heat transfer coefficient, being these two parameters obtained from suitable correlations, and θ_w is the wall temperature. Rigorously, the friction factor and heat transfer coefficient should be determined from the three dimensional solution or from experimental correlations; in practice, values corresponding to hydrodynamic and thermal fully developed conditions are used, neglecting entry length and transient effects. According to Fourier's law and newtonian fluid (with Stoke's hypothesis) constitutive law, respectively the axial heat flux and normal stress can be written as:

$$q_x = -\lambda \frac{\partial \theta}{\partial x} \tag{17}$$

$$\tau_{xx} = \frac{4}{3}\mu \frac{\partial V}{\partial x} \tag{18}$$

where λ and μ are respectively the thermal conductivity and fluid viscosity. After some manipulation of the conservation equations, the following equations can be obtained:

$$\begin{aligned}(\psi + \kappa)\frac{\partial \rho}{\partial t} = &-\frac{1}{A}\frac{\partial}{\partial x}\left[\rho\, V\, (\psi + \kappa)\, A\right] \\ &+ \rho\, V \frac{\partial \psi}{\partial x} + \rho\, V \frac{\partial \kappa}{\partial x}\end{aligned} \tag{19}$$

$$\begin{aligned}p_v \frac{\partial V}{\partial t} = &\frac{1}{A}\frac{\partial}{\partial x}\left(V\, \tau_{xx}\, A\right) - \rho\, V \frac{\partial \kappa}{\partial x} - V\frac{\partial P}{\partial x} \\ &- \tau_{xx}\frac{\partial V}{\partial x} - \tau_{wx}\, V \frac{\mathcal{P}_w}{A} + \rho\, V\, g_x\end{aligned} \tag{20}$$

$$\begin{aligned}\theta \frac{\partial s_v}{\partial t} = &-\frac{1}{A}\frac{\partial}{\partial x}\left(\theta\, s_v\, V\, A\right) - \frac{1}{A}\frac{\partial}{\partial x}\left(q_x\, A\right) \\ &+ \tau_{xx}\frac{\partial V}{\partial x} + \tau_{wx}\, V\frac{\mathcal{P}_w}{A} + V\frac{\partial P}{\partial x} \\ &- \rho\, V \frac{\partial \psi}{\partial x} - q_w \frac{\mathcal{P}_h}{A} + \rho\, \Phi\end{aligned} \tag{21}$$

The balance equations (19) to (21) are power equations (per unit volume) corresponding to each one of the terms that contributes to the time derivative of the total energy per unit volume, namely Eq. (7). The balance equations show the power structure of the system. In the balance equations there can be identified three type of terms: divergence, source and coupling terms. The divergence terms take into account the power introduced in the system through the boundary conditions. The source terms constitute the different power sources, external to

the system. Finally, the coupling terms represent power transfer between the velocity, mass and entropy equations; these coupling terms appear, with opposite signs, in pairs of balance equations.

It is important to notice that, as we started from the PDEs describing the dynamics, all the effects compatible with the one-dimensional approximation are modeled.

The conservation and balance equations obtained in this section can be used for laminar as well as turbulent flows considering the independent variables as mean values; flow regime effects are introduced through the friction factor and the heat transfer coefficient.

3. DISCRETE LEVEL FORMULATION

In this Section the BG-CFD metodology is outlined, in order to present the equations needed to solve any one-dimensional compressible duct flow. Details of the derivations for the general three-dimensional problem can be found in Baliño *et al.* (2006). The description of the flow fields in the domain Ω (see Fig. 2) is made in terms of a finite set of nodal values and interpolation functions, as in the Finite Element Method (Zienkiewicz *et al.*, 2005):

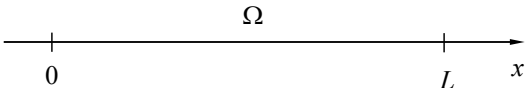

Figure 2: Domain Ω with boundaries.

$$\rho\,(x,\,t) = \sum_{k=1}^{n_\rho} \rho_k\,(t)\;\varphi_{\rho k}\,(x) = \underline{\rho}^T \cdot \underline{\varphi_\rho} \tag{22}$$

$$V\,(x,\,t) = \sum_{m=1}^{n_V} V_m\,(t)\;\varphi_{V m}\,(x) = \underline{V}^T \cdot \underline{\varphi_V} \tag{23}$$

$$s_v\,(x,\,t) = \sum_{l=1}^{n_S} s_{vl}\,(t)\;\varphi_{S\,l}\,(x) = \underline{s_v}^T \cdot \underline{\varphi_S} \tag{24}$$

where $\underline{\rho}$ (size n_ρ), $\underline{V}$ (size n_V) and $\underline{s_v}$ (size n_S) are time-dependent nodal vectors, while $\underline{\varphi_\rho}$, $\underline{\varphi_V}$ and $\underline{\varphi_S}$ are the corresponding position dependent nodal interpolation or shape functions. The interpolation functions have the usual properties: the sum of them is equal to one for any position, they are equal to one at the reference node and are equal to zero at the rest of the nodes. Nodal vectors of integrated values are defined, related to the discretized ones as:

$$\underline{m} = \underline{\underline{\Omega_\rho}} \cdot \underline{\rho} \tag{25}$$

$$\underline{S} = \underline{\underline{\Omega_S}} \cdot \underline{s_v} \tag{26}$$

The diagonal volume matrices $\underline{\underline{\Omega_\rho}}$ and $\underline{\underline{\Omega_S}}$, respectively associated to the density and entropy per unit volume, are defined as:

$$(\Omega_\rho)_{kn} = \Omega_{\rho k}\,\delta_{kn} \tag{27}$$

$$(\Omega_S)_{ln} = \Omega_{Sl}\,\delta_{ln} \tag{28}$$

where:

$$\Omega_{\rho k} = \int_0^L A\,\varphi_{\rho k}\,dx \tag{29}$$

$$\Omega_{Sl} = \int_0^L A\,\varphi_{Sl}\,dx \tag{30}$$

The system mass m and entropy S are related to the integrated variables as follows:

$$m = \int_0^L A\,\rho\,dx = \sum_{k=1}^{n_\rho} m_k \tag{31}$$

$$S = \int_0^L A\,s_v\,dx = \sum_{l=1}^{n_S} S_l \tag{32}$$

3.1 Total energy

The system total energy E is defined as the sum of the system internal energy U and the system kinetic coenergy T^*:

$$E = U\,(\underline{m},\,\underline{S}) + T^*\,(\underline{m},\,\underline{V}) \tag{33}$$

where:

$$E = \int_0^L A\,e_v\,dx \tag{34}$$

$$U = \int_0^L A\,u_v\,dx \tag{35}$$

$$T^* = \int_0^L A\,t_v^*\,dx \tag{36}$$

From Eq. (23) and (36), it can be easily shown that the system kinetic coenergy can be expressed as the following bilinear form:

$$T^* = \frac{1}{2}\,\underline{V}^T \cdot \underline{\underline{M}} \cdot \underline{V} \tag{37}$$

where $\underline{\underline{M}}$ is the system inertia matrix (size n_V, symmetric and regular):

$$(M)_{mn} = \int_0^L A\,\rho\,\varphi_{Vm}\,\varphi_{Vn}\,dx \tag{38}$$

The following potentials are defined:

$$\underline{p} = \left(\frac{\partial T^*}{\partial \underline{V}}\right)_{\underline{m}} = \underline{\underline{M}} \cdot \underline{V} = \int_0^L A\,p_v\,\underline{\varphi_V}\,dx \tag{39}$$

$$\underline{K}\,(\underline{V}) = \left(\frac{\partial T^*}{\partial \underline{m}}\right)_{\underline{\mathbf{V}}} = \underline{\underline{\Omega_\rho}}^{-1} \cdot \left(\int_0^L A\,\kappa\,\underline{\varphi_\rho}\,dx\right) \tag{40}$$

$$\underline{\Theta}\,(\underline{S},\,\underline{m}) = \left(\frac{\partial U}{\partial \underline{S}}\right)_{\underline{m}} = \underline{\underline{\Omega_S}}^{-1} \cdot \left(\int_0^L A\,\theta\,\underline{\varphi_S}\,dx\right) \tag{41}$$

$$\underline{\Psi}\,(\underline{S},\,\underline{m}) = \left(\frac{\partial U}{\partial \underline{m}}\right)_{\underline{S}} = \underline{\underline{\Omega_\rho}}^{-1} \cdot \left(\int_0^L A\,\psi\,\underline{\varphi_\rho}\,dx\right)$$

(42)

where $\underline{p}$, $\underline{K}$, $\underline{\Theta}$ and $\underline{\Psi}$ are respectively nodal vectors of linear momentum, kinetic coenergy per unit mass, temperature and Gibbs free energy per unit mass. The system linear momentum can be readily obtained as:

$$p = \int_0^L A\, p_v\, dx = \sum_{m=1}^{n_V} p_m \tag{43}$$

The time derivative of the system total energy can be written as:

$$\dot{E} = \left(\underline{\Psi} + \underline{K}\right)^T . \underline{\dot{m}} + \underline{p}. \underline{\dot{V}} + \underline{\Theta}^T . \underline{\dot{S}} \tag{44}$$

It can be shown (Baliño *et al.*, 2006) that the constitutive relations $\underline{\Psi} + \underline{K}$, $\underline{p}$ and $\underline{\Theta}$ also satisfy the Maxwell relations.

3.2 State equations

3.2.1 Mass port

Nodal density weight functions $w_{\rho k}\,(x,\, t)$ are introduced. As it is done in the Petrov-Galerkin method (Zienkiewicz *et al.*, 2005), each term of Eq. (19) is multiplied by the weight function; then, the resulting terms are integrated over the domain Ω and Green's theorem is applied in the divergence term, obtaining:

$$\underline{\dot{m}} = \underline{\dot{m}_W^{(\Gamma)}} + \underline{\dot{m}_W} + \underline{\dot{m}_U} + \underline{\dot{m}_K} \tag{45}$$

where the different mass rate nodal vectors are:

$$\begin{aligned}\underline{\dot{m}_W^{(\Gamma)}} = &- \left(\underline{\underline{\Psi}} + \underline{\underline{K}}\right)^{-1} . \Big[A_L\, \rho_L\, (\psi + \kappa)_L\, V_L\, \underline{\delta_{k\, n_\rho}} \\ &- A_0\, \rho_0\, (\psi + \kappa)_0\, V_0\, \underline{\delta_{k\,1}}\Big]\end{aligned} \tag{46}$$

$$\underline{\dot{m}_W} = \left(\underline{\underline{\Psi}} + \underline{\underline{K}}\right)^{-1} . \left[\int_0^L A\, \rho\, (\psi + \kappa)\, V\, \frac{\partial \underline{\underline{w_\rho}}}{\partial x}\, dx\right] \tag{47}$$

$$\underline{\dot{m}_U} = \left(\underline{\underline{\Psi}} + \underline{\underline{K}}\right)^{-1} . \left(\int_0^L A\, \rho\, V\, \frac{\partial \psi}{\partial x}\, \underline{w_\rho}\, dx\right) \tag{48}$$

$$\underline{\dot{m}_K} = \left(\underline{\underline{\Psi}} + \underline{\underline{K}}\right)^{-1} \left(\int_0^L A\, \rho\, V\, \frac{\partial \kappa}{\partial x}\, \underline{w_\rho}\, dx\right) \tag{49}$$

The square matrices $\underline{\underline{\Psi}}$ and $\underline{\underline{K}}$ (size n_ρ) are defined as:

$$(\Psi)_{kj} = \frac{1}{\Omega_{\rho j}} \int_0^L A\, \psi\, w_{\rho k}\, \varphi_{\rho j}\, dx \tag{50}$$

$$(K)_{kj} = \frac{1}{\Omega_{\rho j}} \int_0^L A\, \kappa\, w_{\rho k}\, \varphi_{\rho j}\, dx \tag{51}$$

The nodal vectors $\underline{\Psi}$ and $\underline{K}$ are related to the corresponding matrices as:

$$\Psi_j = \sum_{k=1}^{n_\rho} (\Psi)_{kj} \tag{52}$$

$$K_j = \sum_{k=1}^{n_\rho} (K)_{kj} \tag{53}$$

3.2.2 Velocity port

As it is done in the Galerkin method (Zienkiewicz *et al.*, 2005), each term of Eq. (13) is multiplied by the test function φ_{Vm} and integrated over the domain Ω. Applying Green's theorem in the divergence term, it can be obtained:

$$\underline{\underline{M}} . \underline{\dot{V}} = \underline{F_V}^{((\Gamma)} - \underline{F_K} - \underline{F_P} - \underline{F_V} - \underline{F_{VW}} + \underline{F_G} \tag{54}$$

where the different nodal force vectors are:

$$\underline{F_V^{(\Gamma)}} = A_L\, \tau_{xx\, L}\, \underline{\delta_{m\, n_V}} - A_0\, \tau_{xx\, 0}\, \underline{\delta_{m\, 1}} \tag{55}$$

$$\underline{F_K} = \int_0^L A\, \rho\, \frac{\partial \kappa}{\partial x}\, \underline{\varphi_V}\, dx \tag{56}$$

$$\underline{F_P} = \int_0^L A\, \frac{\partial P}{\partial x}\, \underline{\varphi_V}\, dx \tag{57}$$

$$\underline{F_V} = \int_0^L A\, \tau_{xx}\, \frac{\partial \underline{\varphi_V}}{\partial x}\, dx \tag{58}$$

$$\underline{F_{VW}} = \int_0^L \tau_{wx}\, \mathcal{P}_w\, \underline{\varphi_V}\, dx \tag{59}$$

$$\underline{F_G} = \int_0^L A\, \rho\, g_x\, \underline{\varphi_V}\, dx \tag{60}$$

3.2.3 Entropy port

Nodal entropy weight functions $w_{Sl}\,(x,\, t)$ are introduced. As it is done in the Petrov-Galerkin method (Zienkiewicz *et al.*, 2005), each term of Eq. (21) is multiplied by the weight function; then, the resulting terms are integrated over the domain Ω and Green's theorem is applied in the divergence terms, obtaining:

$$\begin{aligned}\underline{\dot{S}} = &\underline{\dot{S}_Q^{(\Gamma)}} + \underline{\dot{S}_C^{(\Gamma)}} + \underline{\dot{S}_Q} + \underline{\dot{S}_C} + \underline{\dot{S}_{QW}} \\ &- \underline{\dot{S}_U} + \underline{\dot{S}_P} + \underline{\dot{S}_V} + \underline{\dot{S}_{VW}} + \underline{\dot{S}_F}\end{aligned} \tag{61}$$

where the different entropy rate nodal vectors are:

$$\underline{\dot{S}_Q^{(\Gamma)}} = - \underline{\underline{\Theta}}^{-1} . \left(A_L\, q_{x\, L}\, \underline{\delta_{l\, n}} - A_0\, q_{x\, 0}\, \underline{\delta_{l\, 1}}\right) \tag{62}$$

$$\underline{\dot{S}_C^{(\Gamma)}} = - \underline{\underline{\Theta}}^{-1} . \left(A_L\, V_L\, \theta_L\, s_{v\, L}\, \underline{\delta_{l\, n}} - A_0\, V_0\, \theta_0\, s_{v\, 0}\, \underline{\delta_{l\, 1}}\right) \tag{63}$$

$$\underline{\dot{S}_Q} = \underline{\underline{\Theta}}^{-1} . \left[\int_0^L A\, q_x\, \frac{\partial \underline{\underline{w_S}}}{\partial x}\, dx\right] \tag{64}$$

$$\underline{\dot{S}_C} = \underline{\underline{\Theta}}^{-1} . \left[\int_0^L A\, V\, \theta\, s_v\, \frac{\partial \underline{\underline{w_S}}}{\partial x}\, dx\right] \tag{65}$$

$$\underline{\dot{S}_{QW}} = - \underline{\underline{\Theta}}^{-1} . \left[\int_0^L q_w\, \mathcal{P}_h\, \underline{w_S}\, dx\right] \tag{66}$$

$$\underline{\dot{S}_U} = \underline{\underline{\Theta}}^{-1}. \left[\int_0^L A\,\rho\,V\,\frac{\partial \psi}{\partial x}\,\underline{w_S}\,dx \right] \tag{67}$$

$$\underline{\dot{S}_P} = \underline{\underline{\Theta}}^{-1}. \left[\int_0^L A\,V\,\frac{\partial P}{\partial x}\,\underline{w_S}\,dx \right] \tag{68}$$

$$\underline{\dot{S}_V} = \underline{\underline{\Theta}}^{-1}. \left[\int_0^L A\,\tau_{xx}\,\frac{\partial V}{\partial x}\,\underline{w_S}\,dx \right] \tag{69}$$

$$\underline{\dot{S}_{VW}} = \underline{\underline{\Theta}}^{-1}. \left[\int_0^L V\,\tau_{wx}\,\mathcal{P}_w\,\underline{w_S}\,dx \right] \tag{70}$$

$$\underline{\dot{S}_F} = \underline{\underline{\Theta}}^{-1}. \left[\int_0^L A\,\rho\,\Phi\,\underline{w_S}\,dx \right] \tag{71}$$

In Eq. (62) to (71) the temperature matrix $\underline{\underline{\Theta}}$ results:

$$(\Theta)_{lj} = \frac{1}{\Omega_{Sj}} \int_0^L A\,\theta\,w_{Sl}\,\varphi_{Sj}\,dx \tag{72}$$

The nodal vector of temperature is related to the temperature matrix as:

$$\Theta_j = \sum_{l=1}^{n_S} (\Theta)_{lj} \tag{73}$$

4. SYSTEM BOND GRAPH

The system bond graph is shown in Fig. 3. Energy storage (kinetic and potential) are represented by an IC-field. A modulated transformer with the inertia matrix $\underline{\underline{M}}$ is connected to the inertial port of the IC-field, in order to bring the nodal velocities as generalized flow variables.

At the 1-junction with common $\underline{V}$ all the nodal vector forces are added; the effort balance represents the linear momentum conservation equation for the nodal velocity values. At the 0-junction with common $(\underline{\underline{\Psi}} + \underline{\underline{K}})$ all the nodal mass rates are added; the flow balance represents the mass conservation equations for the nodal mass values. At the 0-junction with common $\underline{\Theta}$ all the nodal entropy rates are added; the flow balance represents the entropy conservation equation for the nodal entropy values.

The modulated transformers and the modulated gyrator between the junction elements connect power terms that appear in the balance equations corresponding to pairs of multiports. As the corresponding terms in the balance equations are always positive, the modulated resistance-entropy fields represent the irreversible mechanical energy losses due to viscosity. These elements represent the power coupling terms appearing in Eq. (19) to (21) at a discretized level.

The associated coupling matrix between the velocity and mass port is:

$$\underline{\dot{m}_K} = \left[\left(\underline{\underline{\Psi}} + \underline{\underline{K}}\right)^{-1} . \underline{\underline{M_K}} \right] . \underline{V} \tag{74}$$

$$\underline{F_K} = \left[\left(\underline{\underline{\Psi}} + \underline{\underline{K}}\right)^{-1} . \underline{\underline{M_K}} \right]^T . \left(\underline{\underline{\Psi}} + \underline{\underline{K}}\right) \tag{75}$$

where $\underline{\underline{M_K}}$ is a rectangular matrix (n_ρ rows and n_V columns) defined as:

$$(M_K)_{km} = \int_0^L A\,\rho\,\frac{\partial \kappa}{\partial x}\,w_{\rho k}\,\varphi_{Vm}\,dx \tag{76}$$

The associated coupling matrix between the entropy and mass port is:

$$\underline{\dot{m}_U} = \left[\left(\underline{\underline{\Psi}} + \underline{\underline{K}}\right)^{-1} . \underline{\underline{M_U}} . \left(\underline{\underline{\Theta}}^{-1}\right)^T \right] . \underline{\Theta} \tag{77}$$

$$\underline{\dot{S}_U} = \left[\left(\underline{\underline{\Psi}} + \underline{\underline{K}}\right)^{-1} . \underline{\underline{M_U}} . \left(\underline{\underline{\Theta}}^{-1}\right)^T \right]^T . \left(\underline{\underline{\Psi}} + \underline{\underline{K}}\right) \tag{78}$$

where $\underline{\underline{M_U}}$ is a rectangular matrix (n_ρ rows and n_S columns) defined as:

$$(M_U)_{kl} = \int_0^L A\,\rho\,V\,\frac{\partial \psi}{\partial x}\,w_{\rho k}\,w_{Sl}\,dx \tag{79}$$

Finally, the associated coupling matrices between the velocity and entropy port are:

$$\underline{F_P} = \left(\underline{\underline{\Theta}}^{-1} . \underline{\underline{M_P}} \right)^T . \underline{\Theta} \tag{80}$$

$$\underline{\dot{S}_P} = \left(\underline{\underline{\Theta}}^{-1} . \underline{\underline{M_P}} \right) . \underline{V} \tag{81}$$

$$\underline{F_V} = \left(\underline{\underline{\Theta}}^{-1} . \underline{\underline{M_V}} \right)^T . \underline{\Theta} \tag{82}$$

$$\underline{\dot{S}_V} = \left(\underline{\underline{\Theta}}^{-1} . \underline{\underline{M_V}} \right) . \underline{V} \tag{83}$$

$$\underline{F_{VW}} = \left(\underline{\underline{\Theta}}^{-1} . \underline{\underline{M_{VW}}} \right)^T . \underline{\Theta} \tag{84}$$

$$\underline{\dot{S}_{VW}} = \left(\underline{\underline{\Theta}}^{-1} . \underline{\underline{M_{VW}}} \right) . \underline{V} \tag{85}$$

where $\underline{\underline{M_P}}$, $\underline{\underline{M_V}}$ and $\underline{\underline{M_{VW}}}$ are rectangular matrices (n_V rows and n_S columns) defined as:

$$(M_P)_{ml} = \int_0^L A\,\frac{\partial P}{\partial x}\,\varphi_{Vm}\,w_{Sl}\,dx \tag{86}$$

$$(M_V)_{ml} = \int_0^L A\,\tau_{xx}\,\frac{\partial \varphi_{Vm}}{\partial x}\,w_{Sl}\,dx \tag{87}$$

$$(M_{VW})_{ml} = \int_0^L \tau_{wx}\,\mathcal{P}_w\,\varphi_{Vm}\,w_{Sl}\,dx \tag{88}$$

As the coupling matrices are rectangular, restrictions in the allowable causalities are set.

The source elements connected to the bonds with $\underline{\dot{m}_W^{(\Gamma)}}$, $\underline{F_T^{(\Gamma)}}$, $\underline{\dot{S}_Q^{(\Gamma)}}$ and $\underline{\dot{S}_C^{(\Gamma)}}$ behave as effort or flow sources, depending on the boundary conditions. The rest of the sources represent volumetric power terms; the determination of causality for these sources and for other bonds shown in the graph results from the standard causality extension procedure (Karnopp *et al.*, 2012).

As at any location the sum of the weight functions is equal to one, the net power input (sum over the bonds) corresponding to the multibonds with $\underline{\dot{m}_W}$, $\underline{\dot{S}_Q}$ and $\underline{\dot{S}_C}$ are zero.

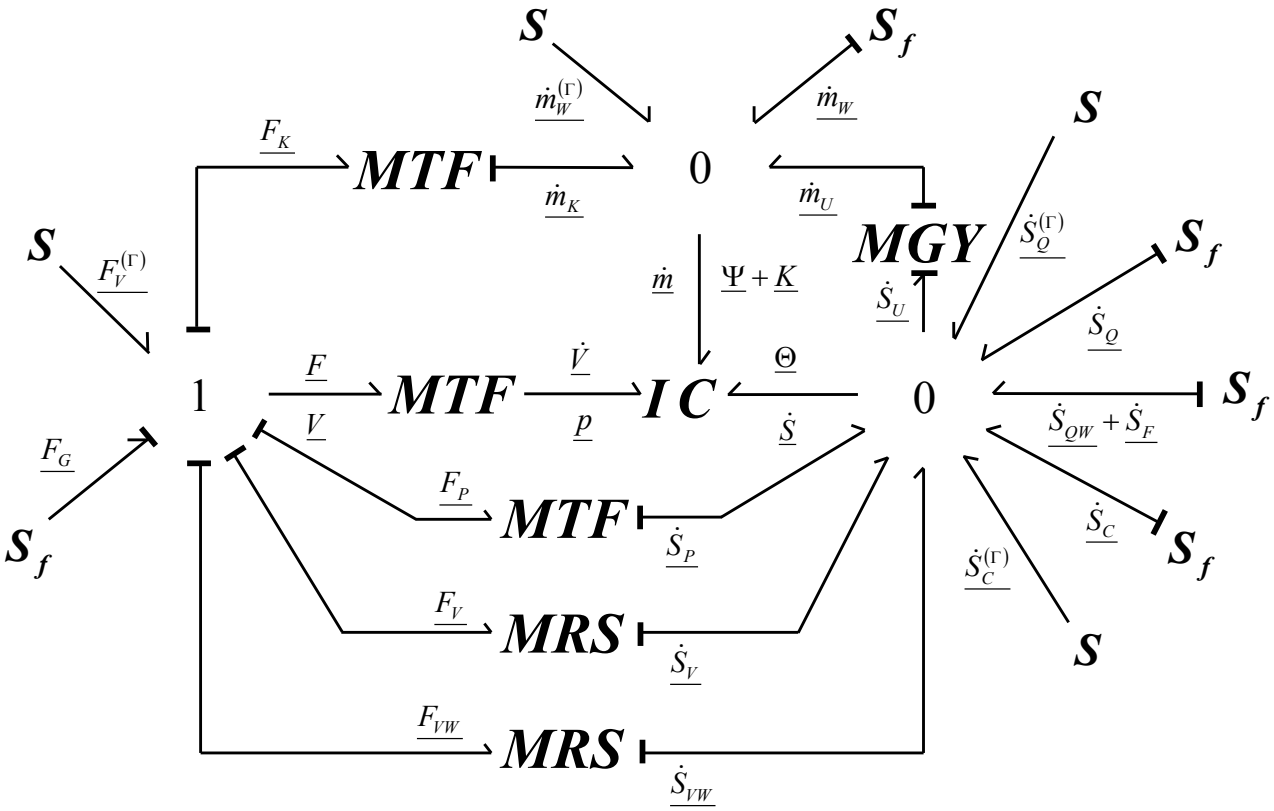

Figure 3: System bond graph for one-dimensional compressible duct flow.

5. CONCLUSIONS

In this paper a Bond Graph methodology described in a previous contribution was used to model compressible one-dimensional duct flows with rigid walls. All physical effects, namely shear wall and normal stresses, wall and axial heat conduction and flow passage area changes can be modeled naturally. Energy storage (kinetic plus internal) can be represented by an *IC*-field. The state equations and the coupling with the inertial and entropy ports were modeled with true bond graph elements. This contribution shows that starting from the governing PDEs equations and using discretization techniques coming from CFD is the right strategy for producing general models, framed within the Bond Graph theory, for Fluid Dynamic Systems.

ACKNOWLEDGEMENTS

This work was supported by Petróleo Brasileiro S. A. (Petrobras). The author wishes to thank *Conselho Nacional de Desenvolvimento Científico e Tecnológico* (CNPq, Brazil).

REFERENCES

Baliño, J. L., Larreteguy, A. E., Gandolfo Raso, E. F., 2001. A General Bond Graph Approach for Computational Fluid Dynamics Part I: Theory. 2001 International Conference on Bond Graph Modeling and Simulation (ICBGM 2001), 41–46.

Baliño, J. L., Larreteguy, A. E., Gandolfo, E. F., 2006. A general bond graph approach for Computational Fluid Dynamics. Simulation Modelling Practice and Theory 14, 884–908.

Baliño, J. L., 2006. Modeling onde-dimensional incompressible duct flows. 20th European Conference on Modelling and Simulation (ECMS 2006), paper 76, 6p.

Baliño, J. L., 2009. Galerkin finite element method for incompressible thermofluid flows framed within the bond graph theory. Simulation Modelling Practice and Theory 17, 35–49.

Borutzky, W., 2010. Bond Graph Methodology. Development and Analysis of Multidisciplinary Dynamic Systems Models. Springer.

Callen, H. B., 1960. Thermodynamics. John Wiley & Sons, Inc..

Fahrenthold, E. P., Venkataraman, M., 1996. Eulerian bond graphs for fluid continuum dynamics modeling. ASME Journal of Dynamic Systems, Measurement, and Control 118, 48–57.

Fletcher, R. H., Tannehill, J. C., Anderson, D. A., 2011. Computational Fluid Mechanics and Heat Transfer. CRC Press.

Gandolfo Raso, E. F., Larreteguy, A. E., Baliño, J. L., 2001. A General Bond Graph Approach for Computational Fluid Dynamics Part II: Applications. 2001 International Conference on Bond Graph Modeling and Simulation (ICBGM 2001), 47–52.

Karnopp, D. C., Margolis, D. L., Rosenberg, R. C., 2012.

System Dynamics: Modeling, Simulation and Control of Mechatronic Systems. Wiley.

Pellegrini, S. P., Baliño, J. L., 2014. Application of a true bond graph formulation for incompressible thermofluid duct flows. 2014 International Conference on Bond Graph Modeling and Simulation (ICBGM 2014), 10 p.

Schapiro, A. V., 1953. The dynamics and thermodynamics of compressible fluid flow. Volume I. The Ronald Press Company, New York.

Zienkiewicz, O. C., Taylor, R. L., Nithiarasu, P., 2005. The Finite Element Method for Fluid Dynamics. Elsevier.

AUTHOR BIOGRAPHY

Jorge Luis Baliño was born in Buenos Aires, Argentina in 1959. He graduated in Nuclear Engineering (1983) and holds the degree of PhD in Nuclear Engineering (1991) from *Instituto Balseiro*, Argentina. He worked for Techint S.A. (1983-1984), *Centro Atómico Bariloche* and *Instituto Balseiro* (1985-2000) in Argentina, *Instituto de Pesquisas Energéticas e Nucleares* (2001-2003) in São Paulo, Brazil. Since 2004 he is Professor at *Universidade de São Paulo*. His research interests are fluid dynamics, heat transfer and multiphase flow.